Supporting information for "Technical note: in-situ measurements and modelling of the oxidation kinetics in films of a cooking aerosol proxy using a Quartz Crystal Microbalance with Dissipation monitoring (QCM-D)"

S1. Description of the KM-SUB kinetic model

We performed model simulations with the kinetic multi-layer model of aerosol surface and bulk chemistry, KM-SUB, using planar geometry. The model's chemical mechanism and kinetic input parameters are based on Berkemeier et al., where the decay of oleic acid was fitted to 12 experimental datasets spanning a range of oxidant concentration and particle size. The model compartments include a gas phase, a near surface gas phase, a sorption layer, a quasi-static surface layer, and a number of bulk layers. The following processes were explicitly resolved in the KM-SUB model: gas phase diffusion of ozone, adsorption and desorption of ozone to and from the sorption layer, surface-bulk exchange, bulk diffusion as well as chemical reactions at the surface and in the bulk of the film. The model code autogenerates a system of ordinary differential equations that represent the mass balance of each chemical species in every model layer. The kinetic model was evaluated for different parameter sets of a fit ensemble (N=167) reported in Berkemeier et al. to represent the uncertainty associated with the global optimization and model extrapolation process. All model input parameters are reported in Berkemeier et al.

S2. Fitting a kinetic model incorporating film growth

The experimental data shows coagulation of droplets upon oxidation. We attempted to model the changes to droplet size over time by including four discrete coagulation events resulting in an increased film thickness and a different surface area to volume ratio (table SX). The model shows the expected slowing of oleic acid decay, which leads to reduced agreement with the experimental data. We speculate that coagulation may have occurred after or towards the end of the oxidation, but for a proper description of this behaviour, time-resolved morphological information is needed.
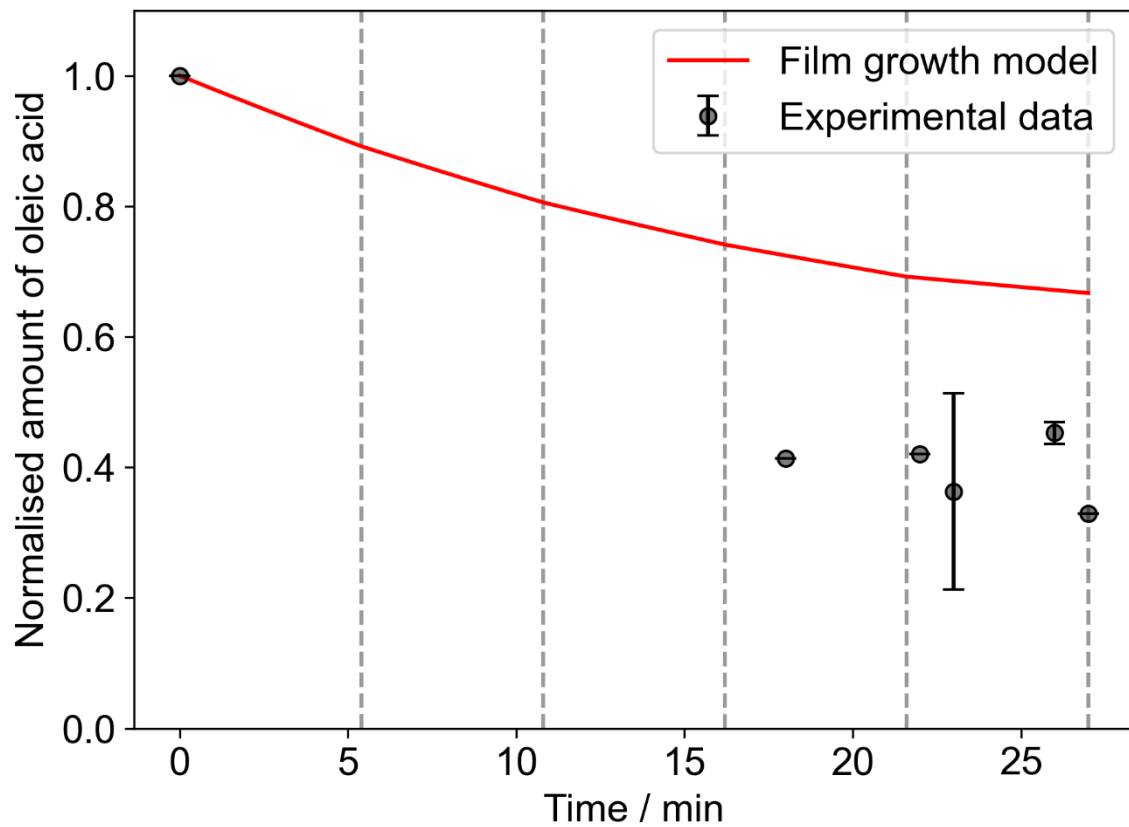
Figure S1. A KM-SUB model analogous to that described in sect. S1 with film thickness increasing after equal time intervals indicated by the vertical dashed lines.

Table S1. Geometry of the film during coagulation events

Model segment	Area (cm^2)	Volume (cm^3)	Thickness (cm)
1	4.0×10^{-5}	2.0×10^{-8}	5.0×10^{-4}
2	1.0×10^{-4}	6.7×10^{-8}	6.7×10^{-4}
3	2.5×10^{-4}	2.2×10^{-7}	8.8×10^{-4}
4	6.4×10^{-4}	7.1×10^{-7}	1.1×10^{-3}
5	1.6×10^{-3}	2.2×10^{-6}	1.4×10^{-3}

S3. Representative height scans of deposited oleic acid before and after ozonolysis
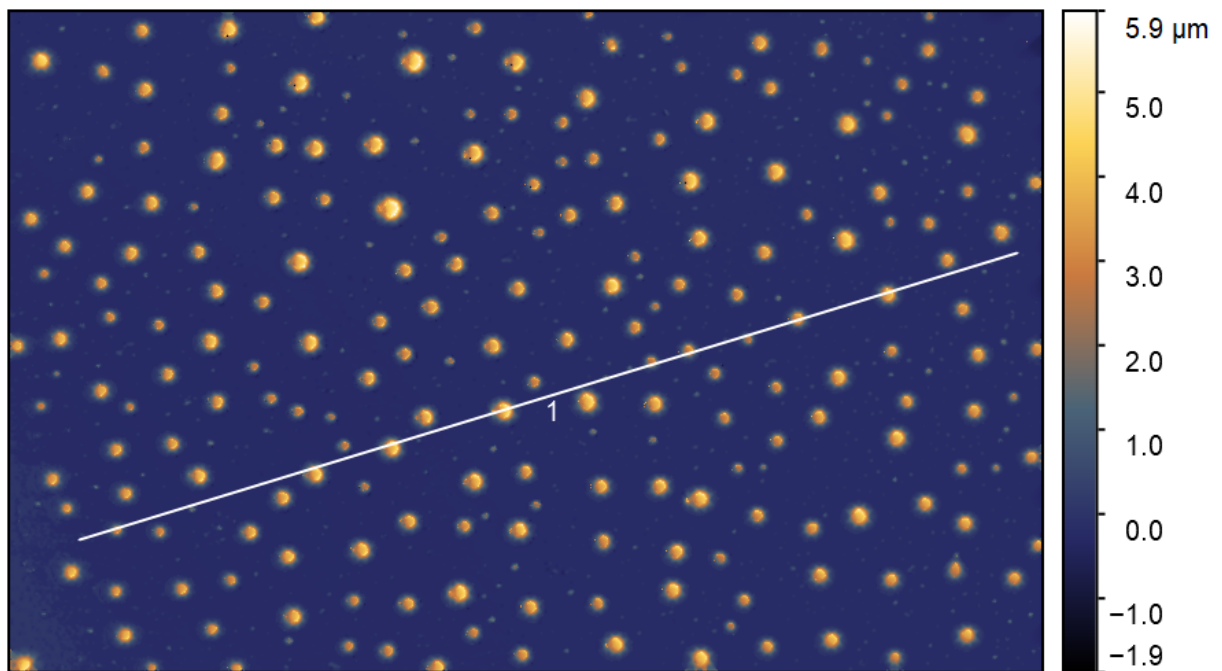
Figure S2. White light interferometry imaging of an oleic acid deposit before ozonolysis. The white line corresponds to the height scan presented in Fig. S3. Deposited on a glass slide.
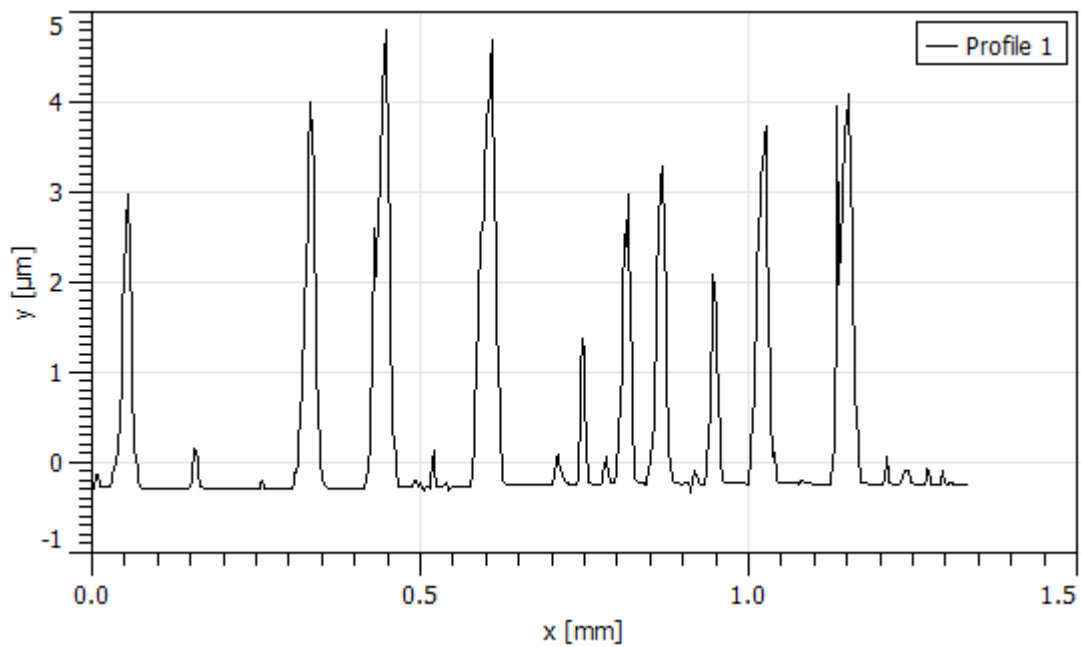
Figure S3. A height scan measured from the image presented in Fig. S2 of an oleic acid deposit before ozonolysis. Deposited on a glass slide.
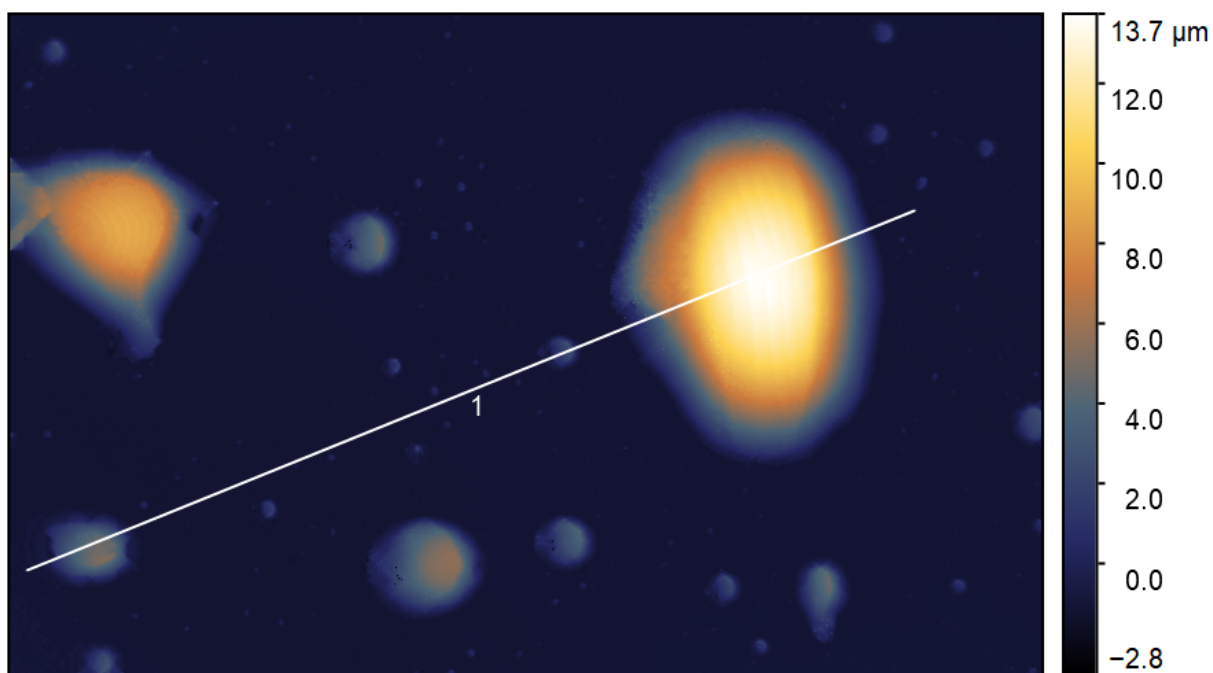
Figure S4. White light interferometry imaging of an oleic acid deposit after ozonolysis. The white line corresponds to the height scan presented in Fig. S5. Deposited on a glass slide.
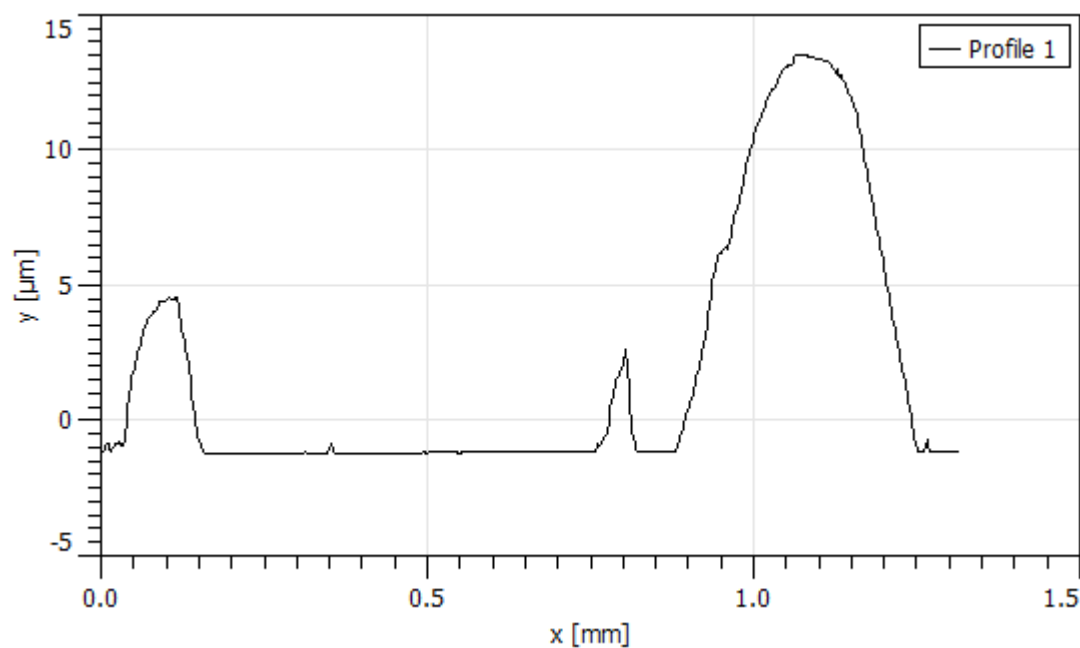
Figure S5. A height scan measured from the image presented in Fig. S4 of an oleic acid deposit after ozonolysis. Deposited on a glass slide.

Reference

T. Berkemeier, A. Mishra, C. Mattei, A. J. Huisman, U. K. Krieger, and U. Pöschl, "*Ozonolysis of Oleic Acid Aerosol Revisited: Multiphase Chemical Kinetics and Reaction Mechanisms*", *ACS Earth Space Chem.*, 2021, 5, 12, 3313–3323.